Aging Propagation in Interconnected Systems with an Application to Advanced Automotive Battery Packs

Andrea Cordoba-Arenas*, Simona Onori**
Giorgio Rizzoni*, Guodong Fan*

** Department of Mechanical Engineering, and Center for Automotive Research, The Ohio State University, Columbus OH, USA, (e-mail:{cordoba-arenas.1;rizzoni.1; fan.267}@osu.edu)*
*** Center for Automotive Research, The Ohio State University, Columbus OH, USA, (e-mail: onori.1@osu.edu)*

Abstract: Real world systems are inherently subject to aging. Aging is the reduction in performance, availability, reliability, and life span of a system or component. The generation of long-term predictions describing the evolution of the aging in time for the purpose of predicting the Remaining Useful Life (RUL) of a system may be understood as Prognosis. The field of prognosis has seen progress with respect to model based and data driven algorithms to model aging and estimate RUL of components. However, in real world applications components are interconnected and aging propagates. Aging propagation from component to others exhibits itself in a reduced system life. Propagation of aging has a profound effect on the accuracy of system SOH assessment and prognosis. This paper introduces a systematic methodology for modeling the propagation of aging in engineering systems, based on the interaction between dynamic system models and dynamic models of damage propagation. The approach is to model the degradation propagation among subsystems that are highly interconnected and tightly integrated within a system. The proposed methodology is applied to advanced automotive battery packs for which different topologies are analyzed and compared in terms of system life.

Keywords: Fault Prognosis, Automotive Systems, Electrified vehicles

1. INTRODUCTION

The supervision of complex engineering systems and processes requires the presence of a variety of diagnostic and prognostic functions to insure three important system properties: 1) **availability**– that is the ability to retain critical system functionality at all times; 2) **safety**– that is the guarantee that under faulty conditions the system will continue to operate in a safe manner, or in compliance with existing regulations; and 3) **serviceability**, that is the assurance that the system can be rapidly serviced or re-configured in the event of one or more malfunctions; this latter property can be of critical importance in the cost-effective operation of a complex network of systems, whether interconnected or individually operated. The three properties are intimately connected to the subject of system **prognosis**.

Real world systems are inherently subject to aging. **Aging** is the reduction in performance, availability, reliability, and life span of a system or component. Aging originates from a number of different case-dependent mechanisms and their interaction. These mechanisms are enhanced by **stress factors** such as load intensity, environmental conditions, and usage patterns. For example, in a battery cell, aging includes capacity decrease and increase in cell impedance; which produce capacity fade and power fade respectively reducing battery performance. Among the micro-mechanisms of battery aging in both positive and negative electrodes, we cite active particle loss and metal sediment or SEI film accumulation. A review on today's knowledge on the mechanics of aging in lithium-ion batteries can be found in (Vetter et al, 2005). These physical-chemical mechanisms are enhanced by stress factors such as current severity (C-rate), operating temperature, state of charge (SOC), cycling rates, overcharge and over-discharge (Vetter et al, 2005; Onori et al, 2012b).

The **state-of-health (SOH)** of a component, which is used to describe its physical condition, is commonly characterized by a system parameter that is correlated with its aging. In most applications, *SOH* is correlated with the performance requirement. Performance requirements depend on the system and its specific application. For example, the requirements for advanced automotive batteries may be ability to store energy, deliver power or a combination of both depending on the intended application. The SOH of a battery cell is commonly characterized by loss in capacity, increase in internal resistance, or a combination of both (Goebel et al. 2008; Onori et al, 2012b).

The generation of long-term predictions describing the evolution of the SOH in time for the purpose of predicting the **Remaining Useful Life (RUL)** of a system may be understood as **Prognosis**. Battery prognosis then refers to the generation of long-term predictions of the evolution of the battery capacity and/or resistance to predict when it will reach a predetermined threshold. Prognosis is one of the key enablers for **Prognostics and Heath Management (PHM).** PHM aims to help in making informed and timely life cycle management decisions, reducing warranty and maintenance costs while improving serviceability, availability and safety.

The field of prognosis has seen progress with respect to model-based and data-driven algorithms to model aging and estimate RUL of components. However, in real world applications components are interconnected and aging propagates from one component to others. In a system, propagation of aging from some components to the others has

a profound effect on the accuracy of system SOH assessment and prognosis.

In (Onori et al. 2012a) the preliminary results of a prognostics methodology for interconnected systems were presented. As a continuation of this work, in this paper a methodology for the analysis of aging propagation in interconnected system under different configurations is proposed and simulation results presented. The methodology is based on the interaction between dynamic system models and dynamic models of damage propagation. The approach is to model the degradation propagation among subsystems that are highly interconnected and tightly integrated within a system. The proposed methodology is applied to advanced automotive battery packs for which different topologies are analyzed and compared in terms of system life.

The rest of the paper is organized as follows; in section 2, the aging modeling for components is described. In sections 3, the methodology for the analysis of aging propagation in interconnected systems is presented. In section 4, the proposed methodology is applied in advanced automotive battery packs. In section 5, simulation results and presented and discussed.

2. AGING MODELING AND SOH FOR COMPONENTS

An engineering component subject to aging can be described by the dynamic equations (1) (Serrao et al, 2009),

$$\begin{aligned} \frac{dx}{dt} &= f_\vartheta(x,\vartheta,u) \\ \frac{d\vartheta}{dt} &= \varepsilon g(\vartheta,p) \\ y &= h_\vartheta(x,\vartheta,u) \end{aligned} \tag{1}$$

- $x \in R^n$ is the set of state variables associated with the fast dynamic behaviour of the component;
- $\vartheta \in R$ is the set of **aging variables**, i.e. the system parameters that change with the age of the component;
- ε is a positive scalar ($\varepsilon << 1$) representing the fact that the dynamics of the aging variables are much slower than the dynamics of the fast variables;
- $u \in R^l$ are the external inputs acting on the component;
- $p \in R^q$ are the aging factors. The vector p can be composed of states and inputs;
- $y \in R^r$ is the component output vector.

To facilitate the analysis of the component aging model, and to permit defining a scalar RUL, we define a mapping function ξ, named **aging measure**, which maps the domain of the system parameters or aging variables onto the scalar domain of aging measure in the interval [0, 1]. For a scalar aging variable, the normalized aging measure can be used to express the progression of the aging process as (Serrao et al 2009),

$$\xi = \frac{\vartheta_f - \vartheta}{\vartheta_f - \vartheta_0} \tag{2}$$

where, $\vartheta_0$is the initial condition of the aging variable (when no aging has taken place) and ϑ_f is the value of the aging variable at the end of life. The SOH of the component, which is used to describe its physical condition, can be characterized by the aging measure ξ. Thus, $SOH = 1$ at the beginning of the component's life, and $SOH = 0$ at end of life. From now on, the terms aging measure ξ and SOH are used interchangeably. A further transformation is needed to represent the fact that aging evolves as a function of the cycling of the system. We define the independent variable *n* as follows:

$$dn = \frac{dt}{T} \tag{3}$$

where T is the time duration of a cycle. Next, we rewrite the aging equation $\dot{\vartheta} = g(\vartheta,p)$ in system (1) in terms of ξ, with n as the independent variable, leading to equation (3):

$$\frac{d\xi}{dn} = \varphi(\xi,p) \tag{4}$$

where φ is the nonlinear map which results from g after the coordinate transformations (2) and (3). Now, the evolution of ξ as given by equation (4) depends on the aging factors *p* and on the present age ξ through the nonlinear function φ. It is known (Todinov, 2001) that if the aging evolution rate $\frac{d\xi}{dn}$, can be factored as the product of a function ρ(ξ) of the current age, ξ, and a function σ(p) of the load, p, that is

$$\frac{d\xi}{dn} = \rho(\xi)\sigma(p) \tag{5}$$

then the Palmgren-Miner can be used to predict the evolution of aging using the additivity law, which states that aging is cumulative , and does not depend on the cycling sequence. We call $\rho(\xi)$ the "age function" and $\sigma(p)$ the "severity factor function". The independent variable *n* is commonly identified with a number of cycles. However, in the case of a battery the concept of cycle is not meaningful because every charge and discharge event is different. For this reason, in a battery *n* is expressed using the total ampere-hour throughput in both charge and discharge, i.e. $n = \int_0^t |I(t)|\,dt$, where $I(t)$ is the input current to the battery (Serrao , 2009). The aging equation that appears in (1) can be written in terms of ξ and the number of cycles n rather than ϑ and time, using equations (3) and (5). Thus the aging model in (1) can be represented by

$$\begin{aligned} \frac{dx}{dt} &= f(x,\xi,u) \\ \frac{d\xi}{dn} &= \rho(\xi)\sigma(p) \\ y &= h(x,\xi,u) \end{aligned} \tag{6}$$

It has been shown experimentally (Serrao, 2009; Todeschini, 2012) that for lithium-ion battery cells equation (5) holds and can be used for prognostics purposes. Recently, the Palmgren-Miner rule has also been used to model aging of electrochemical energy storage by other authors, see for example (Safari, 2010). Ongoing research at OSU CAR has led to the development of cell-level aging models (Serrao, 2009; Todeschini, 2012) that will form the basis for degradation propagation modeling proposed in this work.

3. INTERCONNECTED SYSTEMS SUBJECT TO AGING

3.1 Representation of interconnected systems subject to aging

Let S be a system composed of N components $s_1, s_2, \dots, s_N$, which are subject to aging. When the components are isolated i.e. not interconnected, each component can be modeled according to (6). Therefore, for the *i-th* component:

$$\frac{dx_i}{dt} = f_i(x_i,\xi_i,u_i) \tag{7}$$

$$\frac{d\xi_i}{dn} = \rho_i(\xi_i)\sigma_i(p_i)$$
$$y_i = h_i(x_i, \xi_i, u_i)$$

where, $x_i \in R^{n_i}, \xi_i \in R^N, y_i \in R^{r_i}, u_i \in R^{w_i}$; and f_i and h_i are the state and output nonlinear functions. Upon interconnection, The dynamics of S, which depends on the system's topology, can be represented by equation (9)

$$\begin{aligned} \dot{X} &= F(X, \Xi, U) \\ \frac{d\Xi}{dn} &= \varepsilon G(\Xi, P) \\ Y &= H(X, U) \end{aligned} \quad (8)$$

where;

- $X \in R^n, n = n_1 + n_2 + \cdots + n_N$ is the set of state variables associated with the fast dynamic behavior of the interconnected system, i.e. we assume that the subsystems are disjoint. The set X is the union of sets of state variables of all subsystems. The set X is therefore composed by $x_1, x_2, \dots, x_N$;
$$X = \bigcup_{i=1}^{N} x_i \quad (9)$$
- $\Xi \in R^N$ the set of aging measures for the interconnected system. The set Ξ is the union of the aging variables of all subsystems. The set Ξ is therefore composed by $\xi_1, \xi_2, \dots, \xi_N$;
$$\Xi = \bigcup_{i=1}^{N} \xi_i \quad (10)$$
- F is a possibly nonlinear function of the interconnected system state variables, aging parameters and input that depends on the interconnected systems topology;
- $U \in R^w$ is the set of inputs acting on the interconnected system.
- $Y \in R^r$ is the set of outputs of the interconnected system, it depends on a possible nonlinear function of the interconnected system state variable and inputs;

2.2 Aging Propagation

When an isolated component (i.e. not interconnected) ages its dynamics changes affecting its states and outputs, see (6). Therefore, we can define the aging residual for an isolated component as the difference of its output with no aging, $y_i(t)$ and its output with aging, $y_{i,a}(t)$, i.e. (Onori, 2012a),

$$\Delta y_i = y_i(t) - y_{i,a}(t) \quad (11)$$

This equation can be expressed in terms of the SOH as follows (Onori, 2012a),

$$\Delta y_i = h_i(x_i, \xi_i, u_i) - h_i(x_i, 1, u_i) = \psi_i(\xi_i) \quad (12)$$

When an isolated component is interconnected to other components, the aging residual $\psi_i(\xi_i)$ is propagated through the system and may affect other components dynamics. Therefore, when a component i-th subject to aging is interconnected, the operational conditions (i.e. load intensity, environmental conditions, etc.) of other components as well as the component itself may be affected by the aging of i-th through the interconnection. For example, if the output of the i-th component is the input to the (i-th)+1 component, the aging residual for the downstream component, (i-th)+1, is given by,

$$\begin{aligned} \Delta y_{i+1} &= h_{i+1}\big(x_{i+1}, \xi_{i+1}, y_i + \psi_i(\xi_i)\big) - h_i(x_i, 1, y_i) \\ &= \psi_i(\xi_i, \xi_{i+1}) \end{aligned} \quad (13)$$

and the downstream component aging dynamics are,

$$\begin{aligned} \frac{d\xi_{i+1}}{dn} &= \rho_{i+1}(\xi_{i+1})\sigma_{i+1}(x_{i+1}, y_i + \Delta y_i) \\ &= \rho_{i+1}(\xi_{i+1})\sigma_{i+1}(x_{i+1}, y_i + \psi_i(\xi_i, \xi_{i+1})) \end{aligned} \quad (14)$$

therefore, the severity factor function, σ_{i+1}, is now a function of the SOH of components i and i+1, i.e. $\sigma_{i+1}(\xi_i, \xi_{i+1})$. Meaning, that the aging dynamics of component *i+1* may be affected by the SOH of component *i*, as well as its own SOH.

Modelling aging propagation in interconnected systems faces several challenges. First, the aging dynamics are usually highly nonlinear and may depend of several stress factors. Second, within a system, the interconnections may be due to multiple physical phenomena simultaneously. For example, in a battery pack the interconnections may be electrical, thermal, etc. Third, interconnected systems may be composed of several components, such as in the case of advanced automotive batteries, in which a pack may consist in hundreds of battery cells interconnected under different topologies.

2.3 State-of-health of complex systems: A novel approach

As described in the previous section, the SOH of a component is characterized by its aging measure ξ, Equation (2). Therefore, for the *i-th* component in an interconnected system, the SOH is given by

$$SOH_i = \xi_i \quad (15)$$

At system level, we propose to model the state-of-health of the interconnected system, SOH_{sys}, by a function of its subsystems state of health. The SOH_{sys} is defined based on the system's performance requirement, mode of operation, and topology. Therefore, SOH_{sys} is a possibly nonlinear function of the interconnected components SOH,

$$SOH_{sys} = \xi_{sys} = h(\xi_1, \xi_2, \dots, \xi_N) \quad (16)$$

where $h: R^N \rightarrow [0,1]$. SOH_{sys} is equal to 1 at the beginning of its lifespan and reaches 0 when the system gets to its end-of-life. The task of systematically determine SOH_{sys} from its components, faces important challenges since the system level SOH varies form system to system and it heavily depends on the system mode of operation, intended function, performance requirements, and systems topology.

4. CASE STUDY: ADVANCED BATTERY PACKS

An especially rich example of aging propagation is the case of a battery pack. A battery pack in a hybrid electric vehicle is a collection of modules, which are in turn made up of series/parallel combinations of individual cells. Cells (or modules) are connected in parallel to satisfy high capacity requirements and in series to provide the desired system voltage. Figure 2 depicts a sketch of two possible electrical configurations for a battery module containing the same number of cells. The one on the left is termed "3P8S" because consists of 3 parallel strings of 8 cells in series; the one on the right is termed "8S3P" because consists of 8 elements in series, each consisting of 3 cells in parallel.

Nominally, the two configurations are equivalent in terms of module capacity and output voltage. However, within each module, each cell behaves differently due to manufacturing differences, aging, different operating currents and temperatures, etc. For example, in a string of cells in series, cells see the same current, but the individual cell voltages and states of charge, as well as internal resistance, may vary.

Such imbalances, which are made more pronounced by aging effects, will lead to a faster aging of individual cells, possibly causing an additional load on the other cells and reducing the life of the module and of the pack.

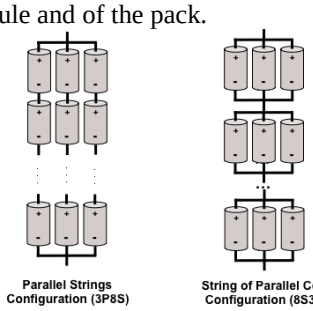

Fig 2. Battery module topologies (*Yurkovich, 2010*)

In this section, the proposed methodology for the analysis of aging propagation is applied to battery modules. The battery modules consist of 10 battery cells. The battery cells are the commercially available A123 ANR26650 cylindrical Li-ion cells, see Figure 3. The battery module geometry is shown in Figure 3. Two equivalent electrical topologies "5S2P" and "2P5S" are analyzed and compared in terms of system (and components) life. The modules are also analyzed under two different applications, power and capacity. We use cell aging models derived from aging experiments on individual cells (Todeschini, 2012). Each cell is modeled in terms of its fast and aging dynamics. An interconnected representation that accounts for thermal and electrical interconnections is used to model the battery modules (system level). The battery pack electro-thermal model is described in the following sub-sections.

(a) (b)

Fig 3. (a) A123 Lithium ion phosphate (LiFePO4) battery cell. Dimensions: diameter (D) =26mm, length (l) =65mm. (b) Battery module geometry, cell #1 is the one located in the top left while cell # 10 is the one located in the bottom right.

3.1 Battery Module Model

Electrical model:

The fast electrical dynamics of each battery cell in the module can be modeled by the 1st order Randle equivalent circuit shown in Figure 4 (Pett, 2004; Hu, 2010). For the cell (index number *i*), the circuit is composed of an ideal voltage source $V_{oc,i}$ to model the cell open circuit voltage, a resistance R_i to model the electrolyte resistance and an RC circuit in series configuration to model the cell electric dynamics ($R_{1,i}, C_{1,i}$). In a cell, the **open circuit voltage** (OCV) is defined as the voltage that is measured with a voltmeter at the terminals of a cell, when there is no current drawn into the battery.

The cell electrical model is given by System (17) where $z_i(t)$ is the cel SoC, $Q_i(t)$ is the cell capacity, $I_i(t)$ is the input current, $V_{c,1}(t)$ is the voltage across the capacitor $C_{1,i}$ and $V_{oc,i}$ is the OVC. The sign of $V_{c,i}$ is selected based on standard current convention (negative current sign for charging and positive current for discharging).

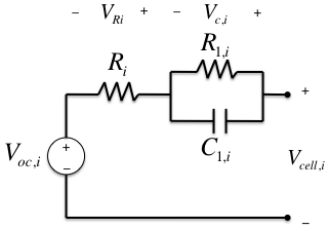

Fig 4. Battery cell electrical model

The OCV is a function of SoC and temperature. All the electrical circuit elements depend on operating conditions (i.e. current, temperature, SoC, charge/discharge) and, the capacity Q_i and resistance R_i vary with the age of the battery.

$$\begin{aligned} \frac{dV_{c,i}}{dt} &= -\frac{1}{R_{1,i}C_{1,i}}V_{c,i} + \frac{I_i}{C_{1,i}} \\ \frac{dz_i}{dt} &= -\frac{I_i}{Q_i} \\ V_{cell,i} &= V_{oc,i} - R_i I_i - V_{c,i} \end{aligned} \tag{17}$$

The input current I_i at each cell is calculated using Kirchhoff's voltage and current laws over the module. Therefore, for each electrical topology ("5S2P" and "2P5S"), I_i is calculated in terms of the input current and cells parameters.

Thermal Model:

The battery cells thermal behaviour is modeled assuming each cell as a lumped thermal mass with uniform temperature throughout it. The energy balance equation for a cell (index number i) is given by

$$M_s c_{p,s} \dot{T}_{s,i} = Q_{cell,i} - Q_{ku,i} - \sum_j Q_{kc,ij}$$

where, $Q_{cell,i}$ is the *i-th* battery cell heat generation, $Q_{kc,i}$ is the *i-th* battery surface convection, $Q_{kc,ij}$ is the *i-th* battery cell-to-cell conduction with its direct neighbours. By direct neighbours we mean the neighbour cells along the horizontal and perpendicular axes only. Hence,

$$M_s c_{p,s} \dot{T}_{s,i} = R_i {I_i}^2 - \frac{(T_{s,i} - T_{f,i})}{R_{u,i}} - \sum_j \frac{(T_{s,i} - T_{s,j})}{R_{c,ij}}$$

where, the effective cell heat capacity $M_s c_{p,s}$ is considered constant, $R_{u,i}$ and $R_{c,ij}$ are convection and conduction thermal resistances respectively. The cell energy balance accounts for heat generation due to Joule heating, heat dissipation from surface convection and heat transfer among cells due to conduction. It has been assumed that the internal resistance *R* is solely responsible for Joule heat generation.

Aging Dynamics:

Capacity fade:

The capacity fade can be modeled as (Todeschini, 2012),

$$C_i(n) = a(SOC_i, T_{s,i}, C_{rate,i}) \cdot n^b \tag{18}$$

where,

$$C_i(n) = \frac{Q_i(n) *}{Q_0} 100$$

where, Q_0 is the cell nominal capacity, $Q_i(n)$ is the i-th cell capacity after n cycles, and $C_i(n)$ is the capacity degradation measure for the *i-th* cell. Therefore, the damage measure in ξ_i, is given by $C_i(n)$. Thus, the aging dynamics associated with the capacity fade are given by

$$\frac{d\xi_i}{dn} = a(SOC_i, T_{s,i}, C_{rate,i}) \cdot b \cdot n^{b-1} \quad (19)$$

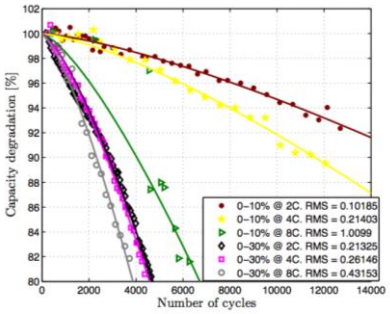

Fig 5. Capacity fade of a Li-ion A123 ANR 26650 battery cell. The fade depends on aging factors such as: SoC of operation, Temperature and C-rate *(Todeschini, 2012)*

Power fade:

The resistance growth can be modeled as (Todeschini, 2012)

$$R_i = R_{0,i} + m_i(SOC_i, T_{s,i}, C_{rate}) \cdot n \quad (20)$$

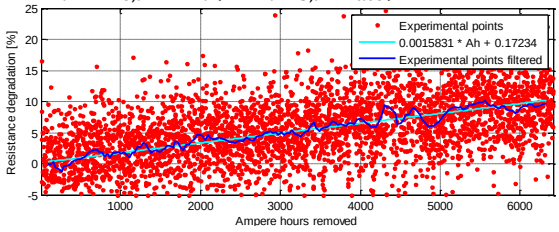

Fig 6. Resistance growth of a Li-ion A123 ANR 26650 battery cell as function of SoC and C-rate. The slope of growth depends on aging factors such as: SoC, Temperature and C-rate (Onori, 2012a)

3.1 Battery module state of health: A novel approach

For electrified vehicles, the battery packs performance requirement depends on the intended application. In HEV applications high power is required to provide adequate boost. In PHEV and EV applications the requirement is mileage range and therefore capacity to store energy. At component level, based on the performance requirement, the SOH of a battery cell is commonly characterized by loss in cell capacity and/or increase in cell internal resistance, parameters correlated with capacity fade and power fade respectively (Goebel 2008; Onori, 2012b). At pack level, however, besides the performance requirement, the system topology also plays an important role in determining SOH_{sys}. In this section, system level SOH_{sys} functions are defined for battery modules intended for capacity applications and two different electrically equivalent topologies ("5S2P" and "2P5S"). Nominally, the capacity of the two battery modules ("5S2P" and "2P5S") is the same (i.e. when all the cells behave identical and no aging occurs, meaning that the cells capacities are all equal). However, due to aging and pack thermal and electrical unbalances, the capacity at each cell is different. Therefore, over time each module will have a different effective capacity. Meaning, that each module and its components will age differently.

Battery pack state of health

Topology aSbP: for a battery module composed of series of cells in parallel (i.e. *a* elements in series consisting of *b* cells in parallel) the module capacity is given by

$$Q_{sys,PS} = \min_{j=1:a} \left(\sum_{i=1}^{b} Q_{i,j} \right) \quad (21)$$

where, $Q_{i,j}$ is the capacity of the cell *i-th* of the *j-th* element.

Topology aPbS: for a battery module composed of parallel strings of cells (i.e. *a* parallel strings composed of *b* cells in series) the module capacity is given by

$$Q_{sys,SP} = \sum_{i=1}^{b} \min_{j=1:a} Q_{i,j} \quad (22)$$

where, $Q_{i,j}$ is the capacity of the cell *i-th* of the *j-th* parallel string. Using equations (21) and (22) with the normalized capacities ξ given by equation (2) (i.e. cells SOH), the battery modules SOH_{sys} can be define for each topology.

5. SIMULATION RESULTS

In this section simulation results of aging propagation within battery packs are presented. In particular, the influence that an aged cell has on the aging of other cells as well as in the pack life is studied. Simulators of the two battery packs described in the previous section (topologies 5S2P and 2S5P) were implemented in MATLAB/Simulink. For each topology, an aged cell with an initial capacity loss of ~4%, is located in cell position # 3, one of the two cells located at the center of the pack (the other one is cell #8, see Figure 3) while all the other cells in the pack are fresh (i.e. zero initial capacity loss). For each topology, the results obtained with the aged cell placed in position #3 are compared with the base-line case of the same pack with all fresh cells. For the simulations presented in this paper, a square-wave current profile of C-rate=2 and period of x seconds, which results in a triangular SOC cell profile (where SOC_{min}= 90% and SOC_{max} =100%), was used as pack current profile.

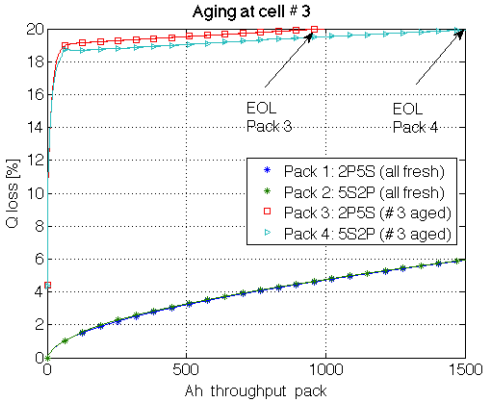

Fig 7. Capacity loss at cell # 3 for different packs

In Figure 7, the capacity loss of cell #3 under the 4 scenarios is shown (Pack 1: 2P5S all cells are fresh, Pack 2: 2P5S all cells are fresh, Pack 3: 2P5S with cell #3 with an initial capacity of ~4%, Pack 4: 2P5S with cell #3 with an initial capacity of ~4%). Similarly the, the capacity loss of cells 8

and 9 are shown in Figure 8 and 9 respectively. As shown in Figure 7, the end-of-life (EOL) of cell #3 depends on the its initial aging as well as on the pack topology. When an aged cell is located in position #3, under topology 5S2P the EOL of cell #3 as well as the pack EOL is reached considerably later that with the 2P5S configuration, (EOL_{5S2P} =1500 Ah, EOL_{2P5S}= 950). Meaning that topology 5S2P is more robust to aging propagation.

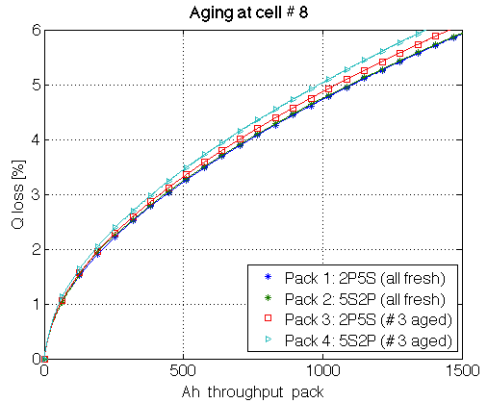

Fig 8. Capacity loss at cell # 8 different packs

As shown in Figures 8 and 9, the aging in cell #3 affects the aging progression of other cells in the pack. The magnitude of aging propagation to other cells depends on the initial aging at cell #3, the pack topology and the cell position within the pack. For example, under the two configurations, the aging of cell #3 propagates to all cells in the pack. However, the propagation effect is most severe on the aging of cell #8. Moreover, the aging of cell #8, is more affected by the aging of cell #3 under the 5S2P topology (see Figure 8). Similar considerations can be made for other cells. For example, for cell #9, whose degradation is more affected by the aging of cell#3 under the 2P5S topology, see Figure 9.

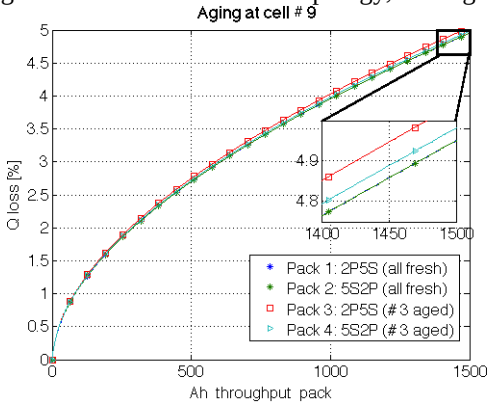

Fig 9. Capacity loss at cell #9 different packs

6. CONCLUSIONS

In this paper a methodology for the analysis of aging propagation in interconnected systems is presented. The proposed methodology shows that the aging progression in a component depend not only of its actual aging and external operation conditions but also, on the aging of other interconnected components. The methodology is applied to advanced automotive battery packs for which different topologies are analyzed and compared in terms of aging propagation and battery pack life.

ACKNOWLEDGEMENTS

The authors acknowledge the valuable contributions to this paper made by Dr. Mutasim A. Salman and Yilu Zhang from General Motors, as well as the financial support of DOE U.S.-China Clean Energy Research Center (CERC).

REFERENCES

Goebel, K., Saha, B., Saxena, A., Celaya, J., Christophersen, J. (2008). Prognostics in Battery Health Management. *Instrumentation & Measurement Magazine*, IEEE, vol.11, no.4, pp.33-40.

Hu, Y., Yurkovich, S., Guezennec, Y., Yurkovich, B.J. (2010). Electro- thermal Battery Model Identification for Automotive Applications. *Journal of Power Sources*, Vol. 196 , pp. 449–457.

Khalil H.K. (2002). *Nonlinear Systems*, Prentice Hall Upper Saddle River, NJ.

Li Z., Lu L., Ouyang, M., Xiao Y., (2011). Modeling the capacity degradation of LiFePO4/graphite batteries based on stress coupling analysis. *Journal of Power Sources*, Volume 196, Issue 22, Pages 9757-9766.

Mahamud, R., Park, C. (2011). Reciprocating air flow for Li-ion battery thermal management to improve temperature uniformity. *Journal of Power Sources*, Volume 196, Issue 13, Pages 5685-5696.

Onori, S., Rizzoni, G., Cordoba-Arenas, A. (2012). A prognostic methodology for interconnected systems: preliminary results. *8th IFAC International Symposium on Fault Detection, Supervision and Safety of Technical Processes, Mexico D.F, Mexico.*

Onori, S., Spagnol, P., Marano, V., Guezennec, Y., Rizzoni, G. (2012). A new life estimation method for Lithium-ion batteries in Plug-in Hybrid Electric Vehicles applications. International Journal of Power Electronics, Vol. 4, 302-319.

Plett, G. (2004). Extended Kalman Filtering for Battery management systems of LiPB-Based HEV battery packs, Part 1: Background. *Journal of Power Sources*, 134, pp.252-261.

Safari, M., Morcrette, M., Teyssot, A., Delacourt, C. (2010). Life Prediction Methods for Lithium-Ion Batteries Derived from a Fatigue Approach. *Journal of the Electrochemical Society*, 157, A892.

Saha, B., Goebel, K., Christophersen J. (2009). Comparison of prognostic algorithms for estimating remaining useful life of batterie. *Transactions of the Institute of Measurement and Control*. Volume (31), 293-308.

Serrao, L., Onori, S., Guezennec, Y., Rizzoni, G. (2009). Model Based Strategy for Estimation of the Residual Life of Automotive Batteries. *7th IFAC International Symposium on Fault Detection, Supervision and Safety of Technical Processes, Barcelona, June 30-July 3.*

Todeschini, F., Onori, S., Rizzoni, G. (2012). An experimentally validated capacity degradation model for Li-ion batteries in PHEVs applications. *8th IFAC International Symposium on Fault Detection, Supervision and Safety of Technical Processes, Mexico D.F, Mexico.*

Todinov, M.T. (2001). *Necessary and sufficient condition for additivity in the sense of the Palmgren–Miner rule.*

Computational Materials Science, Volume 21, Issue 1, Pages 101-110.

Wang, J., Liu, P., Hicks-Garner, J., Sherman, E., Soukiazian, S. and Verbrugge, M. et al. (2011). Cycle-life model for graphite-LiFePO_4 cell. *Journal of Power Sources*, pp.3942–3948.

Yurkovich, B.J. (2010). Electrothermal battery pack model and simulation. *M.S. Thesis, The Ohio State University.*

Vetter, J., Novák, P., Wagner, M.R. , Veit, C., Möller, K.-C., Besenhard, J.O., Winter, M., Wohlfahrt-Mehrens, M., Vogler, C., Hammouche, A. (2005). Aging mechanisms in lithium-ion batteries. *Journal of Power Sources*, Volume 147, Issues 1–2, Pages 269-281.